X-ray absorption studies of some doped mercury cuprate superconductors with varied oxygen stoichiometry

X-ray absorption studies of some doped mercury cuprate superconductors with varied oxygen stoichiometry

B R Sekhar†‡, M Hervieu† and F Studer†

† Laboratoire CRISMAT–CRNS URA1318, ISMRA–Université de Caen, Boulevard du Maréchal Juin, 14050 Caen Cédex, France
‡ Condensed Matter Physics Laboratory, Department of Physics, University of Rajasthan, Jaipur 302 004, India

Abstract. The L_3 x-ray edges of Pr, Pb and Cu in the mixed (Hg, Pr)- and (Hg, Pb)-1212 and 1201 superconductors were studied in order to obtain information about the electronic structure of the (Hg, Pr)– and (Hg, Pb)–O planes and their dependence on O stoichiometry. It has been found that, in Pr doped samples, the average valence of Pr increases with increasing O content. Concomitantly, the density of doping holes increases in the Cu–O planes. In the case of Pb doped samples, the Pb valence was found to be unchanged. We have estimated the density of doping holes per Cu–O plane for these doped Hg superconductors. The results are discussed in view of the band structure calculations in this system.

1. Introduction

The discovery of superconductivity in Hg-based cuprates by Putilin *et al* [1] initiated much interest and research activity in these materials. Although the superconducting members of this family, $HgBa_2Ca_{m-1}Cu_mO_{2m+2+\delta}$, were isolated subsequently [2–9], only a few experimental studies on the electronic structure of these materials have been reported [9–14]. Band structure calculations [15–19] showed that the Fermi surface of Hg-1201 has the shape of a rounded square and that a major Van Hove saddle-point singularity (VHS) exists near the Fermi surface E_F. It was also suggested that an appropriate doping level might be able to move the E_F further to the VHS [16]. As E_F crosses these singular points with change of n_h, a drastic change in T_c may occur [20]. Similar changes were expected in Hg-1212 also, but it was found that the number of doped holes per Cu–O plane per unit cell decreases from Hg-1201 to Hg-1223 [20]. Moreover, these calculations pointed out that the Ba based Hg-1201 behaves like an undoped insulator whereas Hg-1212 and Hg-1223 behave like self-doped systems. Further, it was suggested than an increase in the number of doping holes in the CuO_2 planes may be achieved by introducing more O into the Hg planes [12]. Thus the electronic structure and the changes introduced by doping holes in the system need much more attention than given at present.

Recently, it was shown that the cuprates could be stabilized by the partial substitution of mercury, due to the extraordinary flexibility of the Hg-O layers [2, 7, 8, 21–24]. Elements such as Bi, Pb, Tl and lanthanides and also transition elements such as Ti, V, W, Mo and Cr were found to substitute for Hg in the intermediate layer. The critical temperatures and superconducting volume fractions of the Ba based $(Hg_{1-x}M_x)Ba_2CaCu_2O_{6+\delta}$ are as high as those of pure Hg-1212 superconductors [21]. The Sr based Hg cuprates can

only be stabilized by doping and the $(Hg_{1-x}M_x)Sr_2Ca_{m-1}Cu_m + O_{2m+2+\delta}$ oxides are good superconductors with T_c up to 95 K and high diamagnetic volume fractions. Introduction of Pr has attracted much attention because it proved that Pr rich cuprates can superconduct in contrast to what was observed in Pr doped YBCO. A small amount of Pr was found to decrease the T_c in YBCO monotonically, due to localization of the holes and magnetic pair-breaking interaction, whereas the presence of Pr and Hg-1212 was found to be beneficial for superconductivity. This shows that the roles of Pr in the two compounds are different and deserve a closer look. A detailed study of $Hg_{0.4}Pr_{0.6}Sr_2(A_{1-y}Pr_y)Cu_2O_{6+\delta}$ (A = Sr, Ca) superconductors was reported by Hervieu *et al* [7], where it was shown that Pr atoms occupy two types of crystallographic site. This element is indeed located with Hg in the intermediate layer $[Hg_{0.4}Pr_{0.6}O]$ sandwiched by two [SrO] layers and in the $[A_{1-y}Pr_y]$ layer between the two pyramidal Cu layers. It was also found that Sr based Hg-1201 type cuprates could be stabilized by the introduction of Pr or Pb [8].

The possibility of introducing alien cations with different electronic configurations and oxidation states within the Hg layer is of great interest since this chemical method allows us to easily modify the nature of the Hg plane. Moreover, this flexible layer can adapt an O excess, δ, as the case of Pr cuprates in which the superconducting properties were found to be dependent on the O pressure during synthesis. All these results show that the electronic structure of the Hg-O planes in these doped compounds should be studied in detail. In the same way, a study of the variation in doping hole densities with change in O stoichiometry in doped Hg systems may give more insight into this problem. X-ray absorption spectroscopy (XAS) is a powerful technique for probing the electronic structure of materials and also offers many advantages over other core-level spectroscopies. In XAS, the electronic transitions are governed by dipole selection rules and the reduction in the number of accessible final states facilitates the identification of spectral features [25]. Although this technique has been widely used in the study of high-T_c superconductors, only a few studies have been performed on the new Hg superconductors [12, 13].

This paper presents a study of the electronic structure of some of the Pr and Pb doped Hg-1212 and 1201 superconductors with varied O stoichiometry, using XAS.

2. Experimental details

Different samples were considered for this study, varying the structural type, the Pr or Pb content and the nominal O content. The actual cationic compositions, determined from EDS analyses, structural type and T_c, are given in table 1. These samples were prepared from mixtures of HgO, Pr_6O_{11}, SrO_2, $SrCuO_2$, PbO, La_2O_3, Nd_2O_3 and CaO finely ground in an agate mortar, according to the above formula. The nominal O content was modified by varying the ratio SrO_2–$SrCuO_2$. The samples were heated up to 800 °C in a silica tube; after a plateau of several hours, the temperature was slowly decreased down to room temperature. Details of sample preparation, x-ray diffraction and EDS analysis have been reported earlier [7]. The excess O in these samples has been represented by δ in all the following stoichiometric representations. The superconducting properties were studied using an AC susceptometer (Lakeshore) with an applied field of 5 G.

The x-ray absorption spectra were recorded at room temperature in a classical transmission mode at the EXAFS I station (channel cut monochromator) using the synchrotron radiation of the DCI storage ring of LURE (Orsay, France) working at 1.85 GeV with a 250 mA current.

The normalization procedure used throughout this work was a standard one: after subtraction of the same pre-edge background on the XANES and EXAFS spectra, recorded

Table 1. Pr based cuprates.

No	Structure type	Sample composition [a]	T_c (K)	%Pr(3+)	% Pr(4+) in (Hg, Pr–O) layers	Calculated oxygen content [b]	n_h
1	1212	$Hg_{0.4}Pr_{0.6}Sr_2Sr_{0.7}Pr_{0.3}Cu_2O_{6.45+\delta}$	85	54 ± 1	69 ± 1	6.76	0.11 ± 0.02
2	1212	$Hg_{0.4}Pr_{0.6}Sr_2Sr_{0.5}Pr_{0.5}Cu_2O_{6.55+\delta}$	80	68 ± 1	58 ± 1	6.82	0.10 ± 0.02
3	1212	$Hg_{0.4}Pr_{0.6}Sr_2Ca_{0.5}Pr_{0.5}Cu_2O_{6.55}$	62	68 ± 1	58 ± 1	6.77	0.05 ± 0.02
4	1212	$Hg_{0.4}Pr_{0.6}Sr_2Ca_{0.5}Pr_{0.5}Cu_2O_{6.55+\delta}$	80	60 ± 1	73 ± 1	6.86	0.11 ± 0.02
5	1201	$Hg_{0.4}Pr_{0.6}Sr_2CuO_{4.3+\delta}$	NS	62 ± 1	38 ± 1	4.41	< 0.01

[a] O contents of the samples were calculated assuming all Pr is in 3+ state and Cu is in 2+ state.
[b] O contents of the samples were calculated considering the respective amounts of Pr^{3+}, Pr^{4+}, Cu^{2+} and Cu^{3+} (Cu $3d^9\underline{L}$).

in the same experimental conditions, a point at high energy on the EXAFS spectra, where no more EXAFS oscillations were still observable, was set to unity. Then the intensity of another point on the spectrum, 50–100 eV away from the edge, was determined. Finally, the intensity of a corresponding point on the XANES spectrum with the energy was set equal to that of the latter point.

3. Results and discussion

XAS studies on the samples (Nos 1–8) were performed at three different edges. The L_3 edges of Pr, Pb and Cu have been investigated to evaluate the mean valence of the cations and to obtain qualitative information about the density of doping holes.

3.1. Pr based cuprates: the 1212-type $Hg_{0.4}Pr_{0.6}Sr_2(A_{1-y}Pr_y)Cu_2O_{6+\delta}$ and 1201-type $Hg_{0.4}Pr_{0.6}Sr_2CuO_{4+\delta}$

Four 1212-type cuprates which all exhibit a common Hg–Pr balance in the intermediate layer, i.e. $Hg_{0.4}Pr_{0.6}$, are compared. Samples 1 and 2 differ in the y values which are 0.3 and 0.5, respectively. Sample 4 exhibits the same y value as sample 2 but Sr is replaced by Ca in the perovskite slice. Samples 1, 2 and 4 were prepared under a partial O pressure in the sealed tube (starting from SrO_2). Lastly, sample 3 exhibits exactly the same cationic composition as sample 4 but was prepared under a lower O partial pressure, starting from $SrCuO_2$.

The 1201-type oxide (sample 5) was chosen to present the same composition, $Hg_{0.4}Pr_{0.6}$, of the intermediate layer as that of the above 1212 compounds.

3.1.1. Pr L_3.
The L_3 absorption spectra of Pr in samples 1–5 are shown in figure 1. The figure also shows the L_3-edge absorption spectra of the reference compounds, Pr_2O_3 and PrO_2. These rare-earth oxides have been investigated extensively [25–28] and are classical examples of Pr in trivalency and tetravalency. The L_3 absorption spectra of trivalent Pr exhibit a single absorption line whereas those of tetravalent Pr show a doublet structure. Peak A, in the case of Pr_2O_3, is assigned to the main transitions of 2p → 5d nature. In trivalent compounds of light-rare-earth elements, a weak low-energy shakedown shoulder, 3–4 eV below the main line, has also been observed [29]. In the L_3 absorption spectra of PrO_2, peaks B and C of the doublet are ascribed, following the double-well potential model [25], to the main transitions (2p → 5d) screened by localized and extended 4f states.
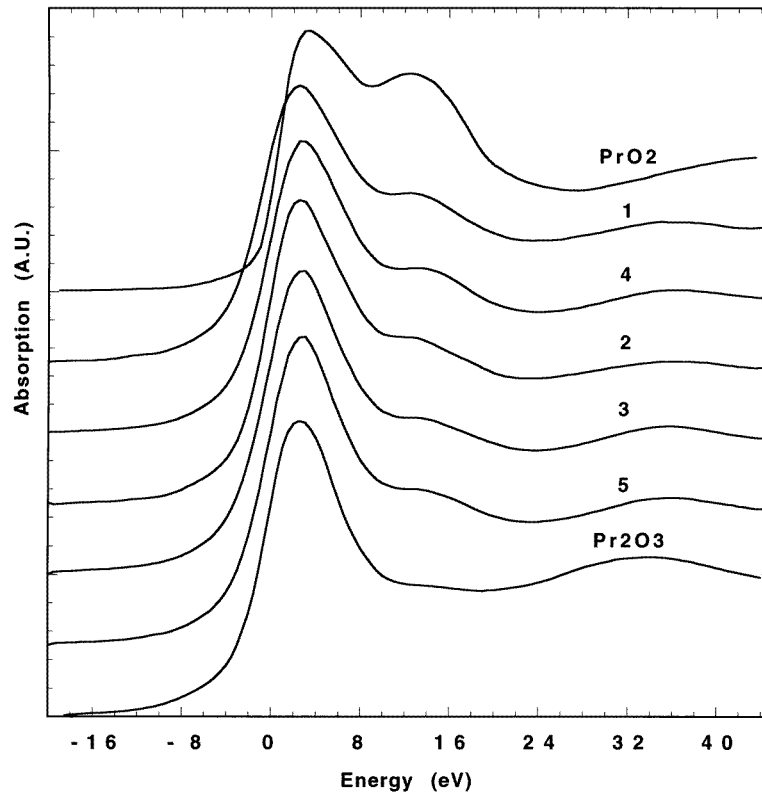
Figure 1. The L_3-edge x-ray absorption of Pr in samples 1–5 along with the corresponding spectra of PrO_2 and Pr_2O_3.

The former states are purely localized whereas the latter states are based on the delocalized Pr (4f–5p–6s)–O (2p) band. In addition to these, in PrO_2, two weak shakedown satellites attached to the main lines B and C have also been observed by Dexpert *et al* [27]. The low-energy peak B is found to be shifted by approximately 2.8 eV on to the higher-energy side with respect to peak A of Pr_2O_3. The L_3-edge absorption spectra of compounds with stoichiometry intermediate between PrO_2 and Pr_2O_3 also have been analysed in detail [25, 26].

In our samples, the L_3 edge of Pr looks more similar to the Pr_2O_3 spectra in shape, but a comparison of the spectra as samples 1–5 to those of the reference compounds would reveal that Pr L_3-edge spectra of these compounds could be deconvoluted into suitably weighted PrO_2 (Pr(4+)) and Pr_2O_3 (Pr(3+)) spectra. Figure 2 shows a typical spectrum deconvoluted into suitably weighted contributions of PrO_2 and PrO_3. The agreement between the spectrum obtained by summing up the contributions from the two reference compounds and the spectrum of sample 1 is satisfactory. This shows that, in these compounds (Nos 1–5), Pr exists in both valence states, Pr(3+) and Pr(4+), and also that the main spectral features could be identified with those coming from PrO_2 and Pr_2O_3. Table 1 shows the results of deconvolution performed on samples 1–5. Table 1 also shows the T_c values of these samples.

It should be remembered here that samples 1–4 have a 1212-type structure while
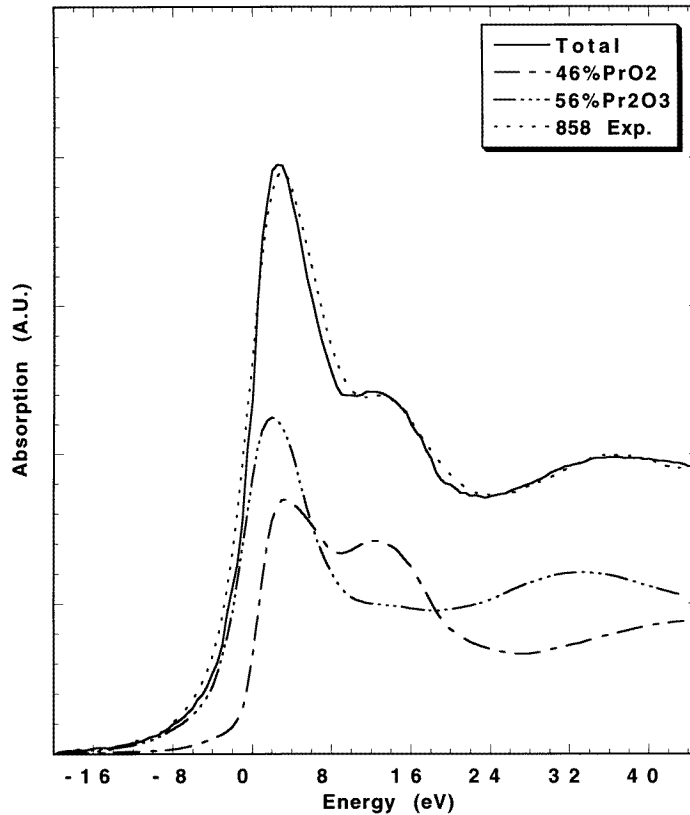
Figure 2. A Pr L_3 spectrum of sample 1 deconvoluted into suitably weighted contributions of Pr L_3 spectra of PrO_2 and Pr_2O_3.

sample No 5 has a 1201 structure. In samples 1–4, Pr occupies some of both the Hg and Sr/Ca sites (in between the $[CuO_2]_\infty$ layers) whereas in sample 5 Pr occupies only some of the Hg sites. A comparison of samples 1 and 2 will show that substitution of more Pr in the Sr site between the $[CuO_2]$ planes results in a significant increase of the Pr(3+) content. This suggests that Pr(3+) occupies preferentially the Sr sites. Replacement of Sr by Ca does not seem to affect the Pr(3+)–Pr(4+) ratio.

The difference in Pr(3+) content in samples 3 and 4 is interesting since it occurs in two samples exhibiting exactly the same cationic composition. Increase in the oxygen stoichiometry (sample 4) coincides with an increase of Pr(4+). This probably shows that the extra O goes to the (Hg, Pr)–O planes, leading to an increase in Pr valence. These results in conjunction with the higher O content and the enhancement of critical temperature suggest that Pr ions located with Ca in the perovskite slice may be in the 3+ valence state whereas those in the Hg–O planes may be in the 4+ valence state. On this assumption, we have estimated the amount of Pr(3+) and Pr(4+) in the (Hg, Pr–O) planes assuming only Pr(3+) ions at the Sr site. The results are given in table 1. It is to be noted that the variations of T_c and the O content appear as correlated to the amount of Pr(4+) in the (Hg, Pr–O) planes.

Our earlier XAS studies [13] on similar samples clearly shows that Hg in this type of
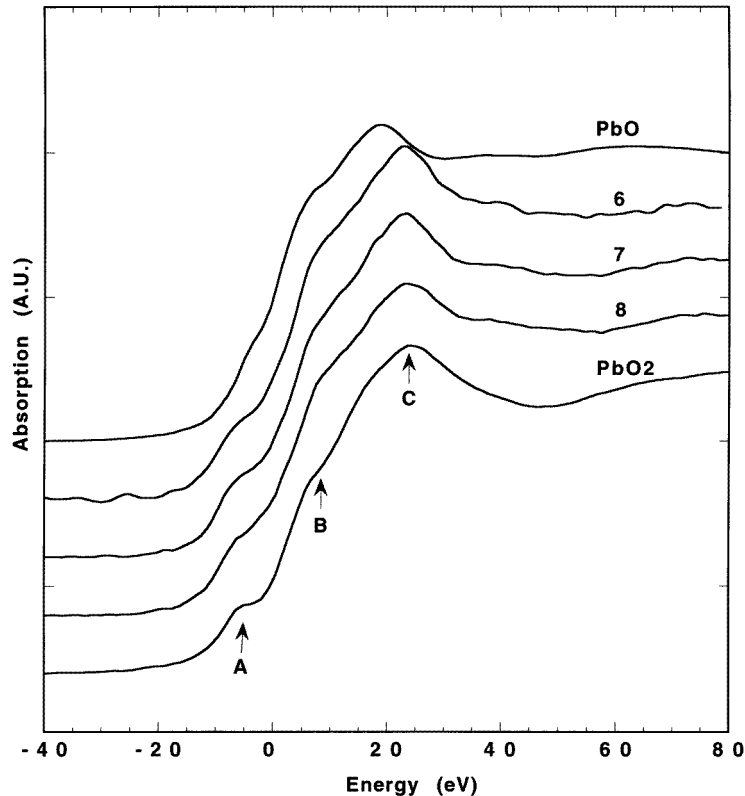
Figure 3. The x-ray absorption spectra of samples 1–5, which include both Cu L$_3$ (931.6) and PrM$_5$ (928.8) edges.

structure exists in an Hg(2+) valence state. Also partial substitution of Bi for Hg results in a mean Bi(4+) formal charge which is well known to be a mixture of Bi(3+) and Bi(5+). Similarly, in this compound Pr may prefer to be in the higher oxidation state while occupying the site in the (Hg, Pr)–O planes. Substitution of Hg(2+) by more Pr(4+) inside the (Hg, Pr)–O planes also may induce more charge transfer of electrons from Pr cations to the O lattice to compensate for the lack of electrons due to Hg(2+). Moreover, this may also result in (Hg, Pr–O) planes acting more as a charge reservoir leading to an increase in the T_c.

3.1.2. Cu L$_3$. Analysis of Cu L$_3$ spectra of cuprate high-T_c superconductors has proved to be an efficient tool for estimating the density of doping holes in the Cu–O planes [30–34]. Unfortunately, the Pr M$_5$ line is found to be almost overlapping with the Cu L$_3$. This makes it difficult to estimate the doping hole densities in Pr containing samples. We tried to subtract the Pr M$_5$ line of these compounds from the total spectra to obtain the Cu L$_3$ line. Figure 3 shows the absorption spectrum which includes both Cu L$_3$ ($\sim$ 931.6 eV) and Pr M$_5$ ($\sim$ 928.8 eV). The Pr M$_5$ spectra for samples 1–5 have been found by adding together the M$_5$ spectra of PrO$_2$ and Pr$_2$O$_3$ in the exact proportions of Pr(4+) and Pr(3+) found by the Pr L$_3$ analysis. Figure 4 depicts the Cu L$_3$ absorption spectrum deduced from
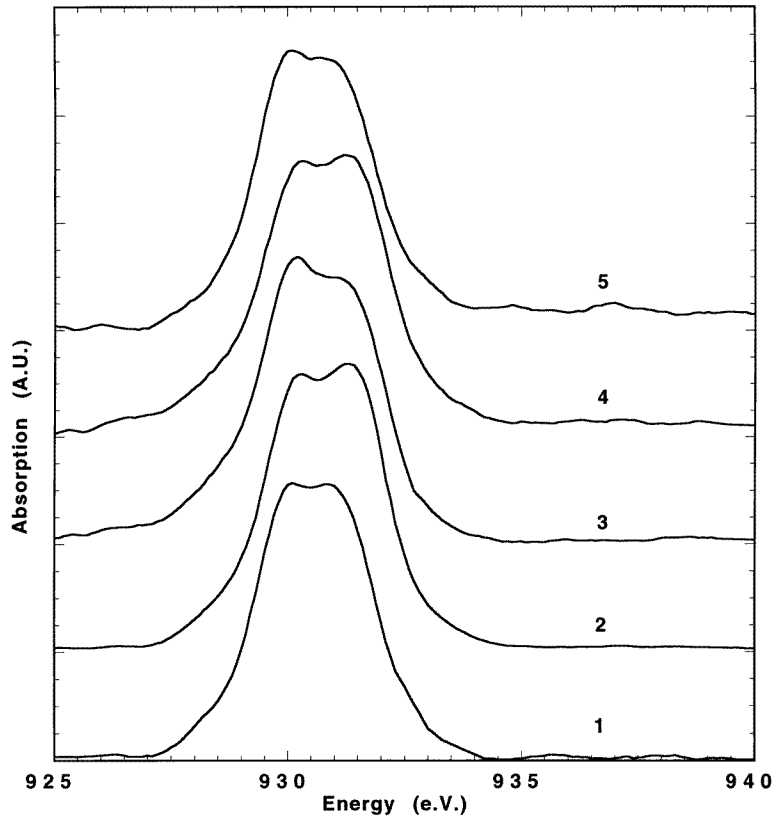
Figure 4. The Cu L_3-edge x-ray absorption spectra of samples 1–5 obtained after subtracting the corresponding M_5 edges of Pr from the spectra of figure 4.

figure 3 for the same set of samples (Nos 1–5). Following the dipole selection rules only the transitions from the Cu $2p_{3/2}$ core level into the unoccupied states of Cu 3d are realized here. The ground state of Cu(2+) can be expressed as $\alpha|3d^9\rangle + \beta|3d^{10}\underline{L}\rangle$, where $|\alpha|^2$ gives the number of Cu 3d holes and $|\beta|^2$ the admixture of empty O 2p states. $\underline{L}$ signifies a hole in the ligand 2p orbitals. Also the ground state of doped cuprates can be expressed as $\gamma|3d^8\rangle + \zeta|3d^9\underline{L}\rangle + \eta|3d^{10}\underline{L}^2\rangle$ and the strong excitonic line at 931.2 eV is due to the $|3d^{10}\rangle$ final state while its shoulder on the high-energy side of 933.2 eV has been assigned to the $|3d^{10}\underline{L}\rangle$ final state of the doped compound [30]. The intensity of this shoulder on the high-energy side provides a good estimate of the doped holes in the CuO_2 planes [30] independently of the nature, localized or delocalized, of the carriers.

The Cu L_3 spectra of samples 1–5 have been deconvoluted into a main line of $3d^9$ and a high-energy shoulder of $3d^9\underline{L}$ as shown previously [30]. A typical fitting of the spectra for sample No 1 is shown in figure 5. From the deconvoluted spectra of the samples we have calculated the mean density of doping holes per copper following the formula

$$n_h = I|3d^9\underline{L}\rangle/(I|3d^9\underline{L}\rangle + I|3d^9\rangle)$$

where I is the intensity of the line. The doping hole densities n_h are also given in table 1. It should be noted that the number of doping holes for the sample with the highest T_c is approximately 0.11. This is in agreement with the earlier reports of 0.12 in optimally doped
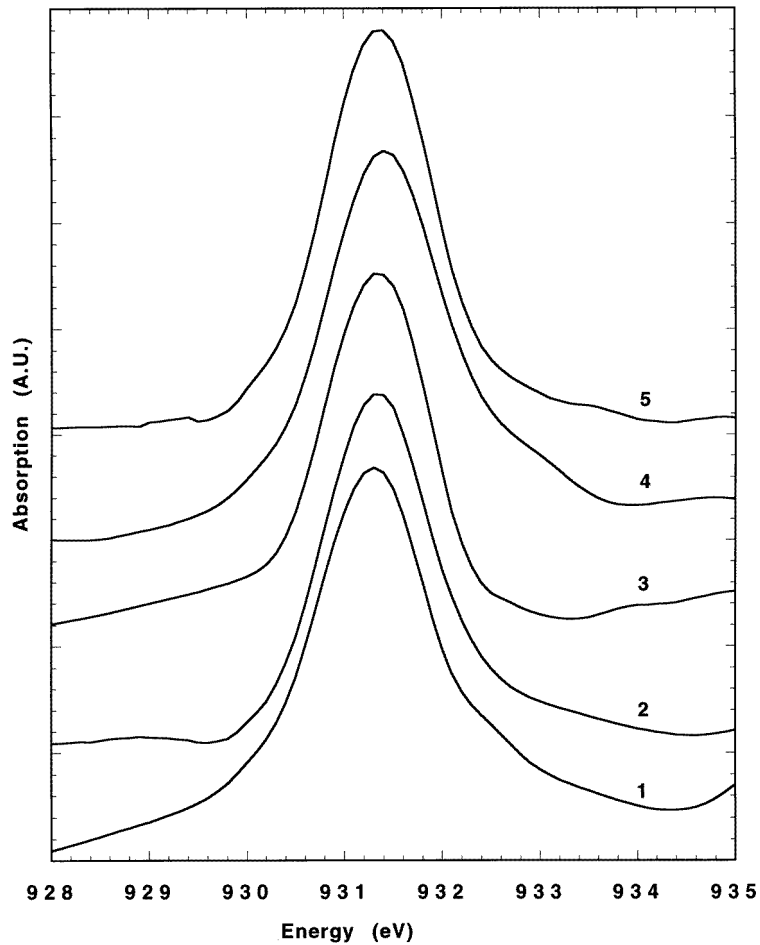
Figure 5. The Cu L_3 spectrum of sample No 1 deconvoluted into a main line of $3d^9$ and $3d^9\underline{L}$.

samples of pure Hg-1212 [12]. It can be seen that for samples 1 and 2 the increase in Pr content at the site in between the Cu–O planes has led to a decrease of T_c. This was expected because, when Pr(3+) replaces Sr(2+), Pr cations supply more electrons to the network, leading to hole filling in the Cu–O planes. The low rate of decrease of T_c and the density of doping holes in the Cu–O planes is again in agreement with the fact that Pr prefers to be in the low-valence state while occupying the site between Cu–O planes. The table also shows that the average formal charge of Cu is the highest in the sample containing the smallest amount of Pr(3+).

The difference in the doping hole densities of samples 3 and 4 is to be noted. The value of n_h is 0.05 for the samples with less O and 0.10 for the one with more O content. Increase in O stoichiometry d has resulted in an increase of T_c and an increase of density of doping holes in the Cu–O planes. This clearly shows that the hole density and the average Cu valence in this compound has a strong dependence on the O stoichiometry. This result is consistent with that of the study of Hg-1212 compound with varied O content by Pellegrin

Table 2. Pb based cuprates.

No	Structure type	Sample composition [a]	T_c (K)	n_h
6	1201	$Hg_{0.3}Pb_{0.7}Sr_{1.4}La_{0.6}CuO_{4.7+\delta}$	40	0.16 ± 0.02
7	1212	$Hg_{0.3}Pb_{0.7}Sr_2Ca_{0.8}Nd_{0.2}Cu_2)_{6.7}$	85	0.13 ± 0.02
8	1212	$Hg_{0.3}Pb_{0.7}Sr_2Ca_{0.8}Nd_{0.2}Cu_2O_{6.7+\delta}$	85	0.12 ± 0.02

[a] O contents of the samples were calculated assuming that the average valence of Pb is 4+.
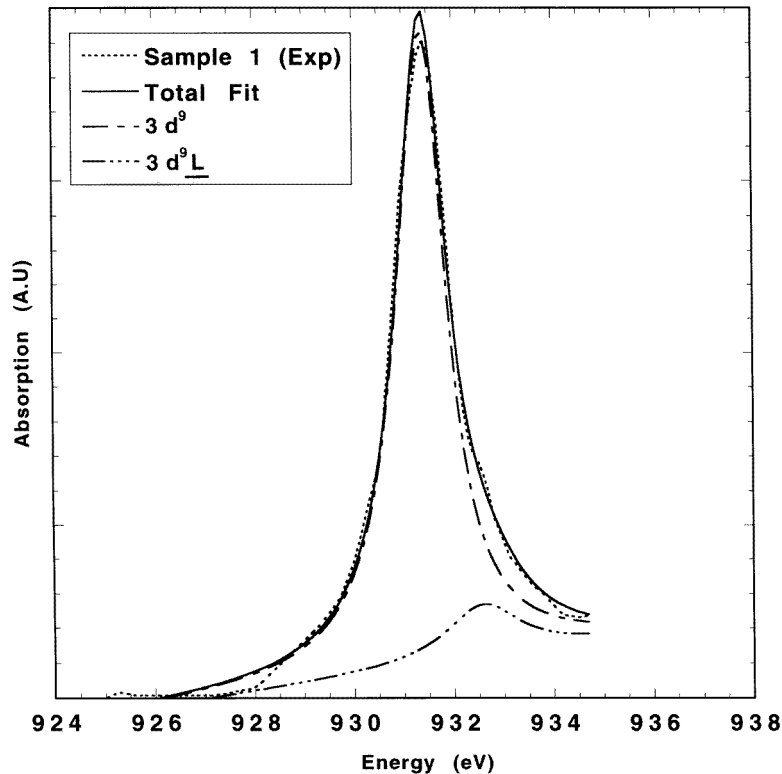
Figure 6. The L_3-edge x-ray absorption spectra of Pb in samples 6–8 along with the corresponding spectra of PbO and PbO_2.

et al [12]. Increase in the O content may increase the O 2p holes within the CuO_2 planes, resulting in an enhanced number of doped Cu–O clusters.

3.2. Pb doped cuprates

For the Pb doped compounds, we select, in the same way, three compounds which correspond exactly to the same composition of the mixed layer, i.e. $Hg_{0.3}Pb_{0.7}$. The two 1212-type cuprates correspond to the same cationic composition and differ only in the oxygen content. Sample 8 was prepared from SrO_2, in contrast to sample 7, but they both exhibit the same T_c. The 1201 compound is La doped and it exhibits a higher T_c.
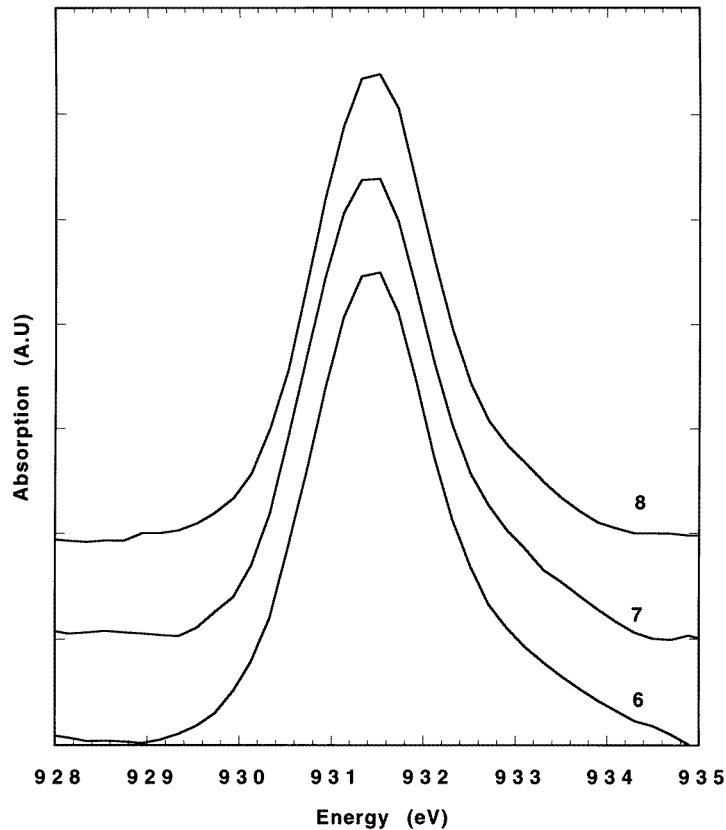
Figure 7. The Cu L_3-edge x-ray absorption spectra of samples 6–8.

3.2.1. Pb L_3.   Table 2 summarizes the results obtained for samples containing Pb in their Hg–O plane. Figure 6 shows the Pb L_3-edge absorption spectra of samples 6–8. Also are shown the corresponding edges of PbO and PbO_2 as reference compounds. The most important difference between the L_3 absorption spectra of PbO and PbO_2 is the presence of a strong pre-peak A which is the signature, at first approximation, of empty 6s levels in PbO_2. This feature allows unambiguous discrimination between Pb(2+) and Pb(4+) valence states [30]. It is quite clear from the figure that peak A is present in the spectra of all the samples numbered 6–8. The peaks C of PbO and PnO_2 are separated by 4.5 eV, which corresponds to crystal field displacements of the lead $6d(e_g)$ levels in these compounds. The position of peak C in our samples 6–8 again shows that Pb is in the higher-valence states in these compounds. This is in agreement with our earlier studies on superconducting cuprates containing Pb [35]. A comparison of samples 7 and 9 reveals that increase in O stoichiometry has not affected the Pb valence. The spectrum of sample 6 shows that Pb occupies the Hg site in Hg-1201 compounds also in the 4+ valence state.

3.2.2. Cu L_3.   Figure 7 depicts the Cu L_3 spectra of the three Pb doped samples. The spectra were deconvoluted in the main line $3d^9$ and a high-energy shoulder of $3d^9\underline{L}$. The deconvoluted spectrum of sample 6 is shown in figure 8. As in the Cu L_3 analysis of Pr
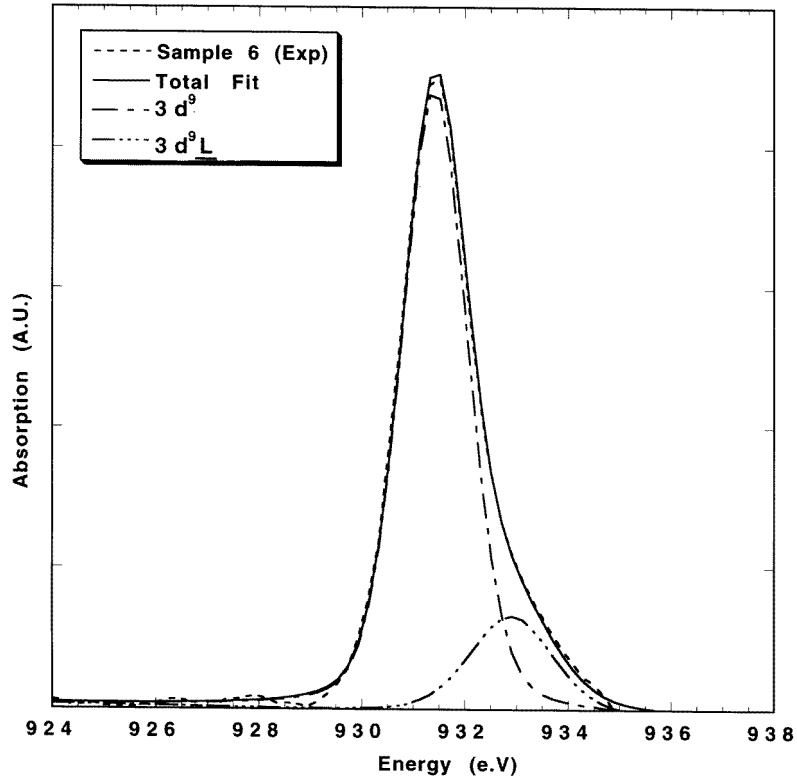
Figure 8. The Cu L_3 spectrum of sample No 6 deconvoluted into a main line of $3d^9$ and $3d^9\underline{L}$.

doped samples, we have calculated the density of doping holes per Cu for these samples also. The results are given in table 2. Sample No 6 shows a comparatively low T_c and a high value of n_h. This value is comparable to that published by Pellegrin *et al* [12] for pure Hg-1201 samples. The small difference may be due to the presence of Pb in the Hg–O planes. Also the low T_c value indicates that probably the optimum value of n_h is smaller than 0.16 and that this compound, perhaps, is overdoped. This result is in accordance with our previous work [36] on Tl(2201), which showed that in single-Cu-layered structures the highest T_c is obtained for $n_h \approx 0.10$. A large value of n_h indicates a high density of doping holes in the Cu–O planes of this sample. The values of n_h are almost equal for samples 7 and 8. It can be seen that variation in O content has not affected the density of doping holes or the T_c in these samples.

4. Concluding remarks

The changes in the critical temperature with the variation of mixed layer nature in the doped $Hg_{1-x}M_x)Sr_2A_{m-1}Cu_mO_{2m+2+\delta}$ cuprates with M = Pr and Pb and A = Sr, Ca or Pr can be understood on the basis of their XAS study. The influence of the alien cation substituting for Hg clearly appears whereas that of the alkaline earth A seems to be very small. The density of holes and T_c increase with increasing O content δ in Pr doped samples while they are not affected in Pb doped samples. This means that increasing the O content within

the (Hg, Pr–O) planes is accompanied by an increase in the density of holes in the Cu–O planes and consequently the T_c, as pointed out by the band structure calculations [17, 18]. It is also quite probable that in these samples the excess O concentration δ is able to move the Fermi level E_F to the nearby VHS. This is in accordance with the band picture proposed by Novikov and Freeman [15]. This may also show that in Pr doped samples the increase in the valence state of Pr with increasing δ could have changed the position of the band arising from hybridized $Hg(5d_{z^2}–6p_z–O\ 2p_z)$ states.

To summarize, we have determined the density of doping holes per Cu–O plane in Pr and Pb doped Hg-1201 and Hg-1212 compounds. In samples doped with Pr an increase in the average valence of Pr coincides with the increase in T_c and hole density in the $[CuO_2]$ planes, whereas for Pb doped samples no change could be observed. In both Hg-1201 and Hg-1212, Pr was found to be in a mixed state of Pr(3+)–(4+) with Pr(3+) occupying the sites in between the $[CuO_2]$ planes and Pr(3+)–Pr(4+) in the Hg–O planes. Pb occupies the site in the Hg–O planes in the Pb(4+) state. This study presents experimental evidence for an increase in the number of doped holes in the $[CuO_2]$ layers when excess O is inserted into the Hg–O planes.

Acknowledgment

References

[1] Putilin S N, Antipov E V, Chmaissen O and Marezio M 1993 *Nature* **362** 266
[2] Pelloquin D, Michel C, van Tendeloo G, Maignan A, Hervieu M and Raveau B 1993 *Physica* C **214** 87
[3] Pelloquin D, Hervieu M, Michel C, Van Tendeloo G, Maignan A and Raveau B 1993 *Physica* C **216** 257
[4] Goutenoire F, Daniel P, Hervieu M, Van Tendeloo G, Michel C, Maignan A and Raveau B 1993 *Physica* C **216** 243
[5] Hu S F, Jefferson D A, Liu R S and Edwards P P 1993 *J. Solid State Chem.* **103** 280
[6] Martin C, Hervieu M, Huve M, Michel C, Maignan A, Van Tendeloo G and Raveau B 1994 *Physica* C **222** 19
[7] Hervieu M, Van Tendeloo G, Maignan A, Michel C, Goutenoire F and Raveau B 1993 *Physica* C **216** 264
[8] Goutenoire F, Daniel P, Hervieu M, Van Tendeloo G, Michel C, Maignan A and Raveau B 1993 *Physica* C **216** 243
[9] Hahakura S, Shimoyama J, Shiino O and Kishio K 1993 *Physica* C **233** 1
[10] Vasquez R P, Rupp M, Gupta A and Tsuei C C 1995 *Phys. Rev.* B **51** 15 657
[11] Almeras P, Dell'Orto T, Coluzza C, Almeida J, Margaritondo G, Xue Y Y, Meng R L and Chu C W 1994 *J. Appl. Phys.* **76** 1100
[12] Pellegrin E, Fink J, Chen C T, Xiong Q, Lin Q M and Chu C W 1996 *Phys. Rev.* B **53** 2767
[13] Studer F, Pelloquin D, Maignan A, Michel C, Hervieu M and Raveau B 1995 *Physica* C **242** 1
[14] Pelloquin D, Michel C, Hervieu M, Studer F and Raveau B 1996 *Physica* C **257** 195
[15] Novikov D L and Freeman A J 1993 *Physica* C **212** 233
[16] Novikov D L, Mryasov O N and Freeman A J 1994 *Physica* C **222** 38
[17] Singh D J, 1993 *Phys. Rev.* B **48** 3571
[18] Singh D J 1993 *Physica* C **212** 228
[19] Rodriguez C O, Christensen N E and Peltzer y Blanca E L 1993 *Physica* C **216** 12
[20] Chen F, Huang Z J, Meng R L, Sun Y Y and Chu C W 1993 *Phys. Rev.* **48** 16 047
[21] Maignan A, Pelloquin D, Malo S, Michel C, Hervieu M and Raveau B 1995 *Physica* C **243** 233
[22] Maignan A, Michel C, van Tendeloo G, Hervieu M and Raveau B 1993 *Physica* C **216** 1
[23] Maignan A, Hervieu M, Martin C, Michel C and Raveau B 1994 *Physica* C **232** 15
[24] Chmaissem O and Sheng Z Z 1995 *Physica* C **242** 23
[25] Karnatak R C 1993 *J. Alloys and Compounds* **192** 64

[26] Gasgnier, Shiffmacher G, Albert L, Caro P E, Dexpert H, Estava J M, Blancard C and Karnatak R C 1989
     J. Less-Common Met. **156** 59
[27] Dexpert H, Karnatak R C, Esteva J M, Connerade J P, Gasgnier M, Caro P E and Albert L 1987 *Phys. Rev.*
     B **36** 1750
[28] Karnatak R C, Estava J M, Dexpert H, Gasgnier M, Caro P E and Albert L 1987 *Phys. Rev.* B **36** 1745
[29] Bianconi A, Marcelli A, Davoli I, Stizza S and Campagna M 1984 *Solid State Commun.* **49** 409
[30] Studer F, Michel C and Raveau B 1993 *Mater. Sci. Forum* **137** 187
[31] Bianconi A *et al* 1988 *J. Phys. C: Solid State Phys.* **9** 179
[32] Kuiper P, Kruizinga G, Ghijsen J, Sawatzky G A and Verweij H 1989 *Phys. Rev. Lett.* **62** 221
[33] Fink J *et al* 1990 *Proc. Int. School Mater. Sci. Technol. (Erice 1989) Earlier and Recent Aspects of
     Superconductivity* ed K A Muller and G Bednorz (Berlin: Springer) p 377
[34] Tolentino H, Dartyge E, Fontaine A, Tourillon G, Gourieux T, Krill G, Maurer M and Ravet M F 1989 *Proc.
     Int. Symp. on the Electronic Structure of high T_c Superconductors (Rome 1988)* ed A Bianconi (Oxford:
     Pergamon)
[35] Studer F, Bourgault D, Martin C, Retoux R, Michel C and Raveau B 1989 *Physica* C **159** 609
[36] Merrien N, Coudrier L, Martin C, Maignan A, Studer F, and Flank A M 1994 *Phys. Rev.* B **49** 9906